Molecular Vision 2019; 25:535-545 <http://www.molvis.org/molvis/v25/535>
Received 24 April 2019 | Accepted 3 July 2019 | Published 3 October 2019

CHOP is dispensable for lens transparency in wild-type and connexin50 mutant mice

Peter J. Minogue, Eric C. Beyer, Viviana M. Berthoud

Department of Pediatrics, University of Chicago, Chicago, IL

Purpose: CCAAT/enhancer-binding homologous protein (CHOP), a transcription factor that has been implicated in differentiation, apoptosis, and autophagy, is greatly elevated in lenses with cataracts due to mutations of several different lens proteins. To test the possible role of CHOP in the cataractous lens, we studied the effect of knocking out *Chop* in mice that were homozygous for the Cx50D47A mutation of the lens fiber gap junction protein connexin50 (Cx50).
Methods: Mouse lenses were examined by dark-field microscopy. Lens equatorial diameters and intensities of the opacities were quantified using ImageJ. Transcript levels were assessed by real-time quantitative PCR. Protein levels were determined by immunoblotting.
Results: Homozygous *Chop* knockout lenses were transparent. Deletion of *Chop* in Cx50D47A mice did not improve lens transparency and had no effect on lens size. In *Chop* null-Cx50D47A lenses, the protein kinase R–like endoplasmic reticulum kinase (PERK)-dependent pathway was activated similarly to Cx50D47A lenses. In Cx50D47A mice, *Chop* deletion did not improve connexin levels or lens fiber cell differentiation, and it did not decrease the levels of *Trib3* or *Irs2* transcripts to wild-type values. However, homozygous *Chop* knockout significantly diminished the increased levels of *Cebpb* transcripts of Cx50D47A lenses.
Conclusions: The results show that CHOP is not required for lens transparency. They also suggest that CHOP is not the critical etiological factor for the cataracts observed in homozygous Cx50D47A lenses, further supporting a major role for connexins in the disease.

Congenital cataracts are a major cause of visual impairment and blindness in infants and young children (reviewed in [1]). Often, they result from mutations in different genes, including those encoding crystallins, transmembrane proteins, transcription factors, and extracellular matrix proteins (compiled in Cat-Map) [2]. Among the transmembrane proteins, mutations in the lens fiber cell gap junction proteins, connexin46 (Cx46) and connexin50 (Cx50), are common. We have been studying mice expressing one such mutant, Cx50D47A, as a prototype of connexin-linked cataracts. Both heterozygous and homozygous Cx50D47A mice develop cataracts [3-5]. The lenses of these mice are small, and fiber cell differentiation is impaired [3]. In the mutant lenses, the protein kinase R–like endoplasmic reticulum kinase (PERK) transducing pathway of endoplasmic reticulum (ER) stress is activated [6]. This response is most severe in homozygotes, as shown by phosphorylation of eukaryotic translation initiation factor-2A (EIF2α) and increased protein levels of activating transcription factor 4 (ATF4) and its downstream target, CCAAT/enhancer-binding homologous protein (CHOP). We hypothesized that persistent activation of this pathway may contribute to the impaired differentiation and cataract formation in Cx50D47A mice. CHOP is also significantly increased in lenses containing cataracts, including those caused by mutations of other genes [7-10], suggesting that CHOP may be a general critical factor that contributes to these abnormalities.

CHOP (also known as DNA damage inducible transcript 3, DDIT3; C/EBPζ; and growth arrest and DNA damage protein, GADD153) is a transcription factor that can be induced by physiological conditions and a wide variety of cellular stresses (including ER stress; reviewed in [11,12]). Studies in various cell types suggest that CHOP has a critical role in the induction of cell cycle arrest and apoptosis in response to stress. CHOP has been implicated in regulating apoptosis, autophagy, and cell differentiation (reviewed in [12]). It can dimerize with other transcription factors and act as a negative or positive regulator of transcription, depending on its transcription factor partner, the cell type, and the stress condition ([13]; reviewed in [14]). Our prior investigation of Cx50D47A lenses showed large increases in some transcripts that could result from CHOP-mediated transcriptional activity (including *Trib3*). Therefore, we sought to investigate the importance of CHOP in the lens by studying the effects of deleting CHOP from wild-type mice and homozygous Cx50D47A mice.

Correspondence to: Viviana M. Berthoud, Department of Pediatrics, University of Chicago, 900 East 57th St., KCBD-5150, Chicago, IL 60637; Phone: (773) 834-2115; FAX: (773) 834-1329; email: vberthou@peds.bsd.uchicago.edu

Table 1. List of real-time quantitative PCR primers.

Target RNA	Primer sequence (5'-3')
Chop	F: CTGCCTTTCACCTTGGAGAC
	R: CGTTTCCTGGGGATGAGATA
Total *Xbp-1*	F: GAACCAGGAGTTAAGAACACG
	R: AGGCAACAGTGTCAGAGTCC
Spliced *Xbp-1*	F: AGCTTTTACGGGAGAAAACTCA
	R: GCCTGCACCTGCTGCG
Trib3	F: TGGCTGGCAGATACCCATTC
	R: CAAGTCGCTCTGAAGGTTCCTT
Irs2	F: GGGGCGAACTCTATGGGTA
	R: GCAGGCGTGGTTAGGGAAT
Cebpb	F: GGTTTCGGGACTTGATGCA
	R: CAACAACCCCGCAGGAAC
Cyclophilin A	F: TATCTGCACTGCCAAGACTG
	R: ACAGTCGGAAATGGTGATCT

F represents forward primer, R represents reverse primer.

METHODS

Chemicals: KCl, Ponceau S, 1,2-Bis(dimethylamino)ethane (TEMED), 2-mercaptoethanol, Trizma base and glycine were obtained from Sigma-Aldrich (St. Louis, MO). NaCl, KH_2PO_4, Na_2HPO_4*7 H_2O, ethylenediaminetetraacetic acid disodium salt dihydrate, ProtoGel, sodium dodecyl sulfate and methanol were obtained from Thermo Fisher Scientific (Pittsburgh, PA). Ammonium persulfate was obtained from Bio-Rad (Hercules, CA). ProSieve QuadColor™ protein markers (4.6 kDa – 300 kDa) were obtained from Lonza Rockland, Inc. (Rockland, ME).

Antibodies: Mouse monoclonal anti-CHOP (9C8) antibody (MA1–250; lot # QG214389) was obtained from Thermo Fisher Scientific. Rabbit monoclonal anti-EIF2α (D7D3) (5324P; lot # 3), anti-P-EIF2α (Ser51) (D9G8) XP (3398P; lot# 2), anti-histone H3 (D1H2) XP (4499S; lot # 9), and anti-calreticulin (CALR) (DE36) (12238S; lot # 4) antibodies were obtained from Cell Signaling Technology (Danvers, MA). Rabbit polyclonal anti-translocase of outer mitochondrial membrane 20 (TOM20) antibodies (FL-145; sc-11415; lot # D1613) were obtained from Santa Cruz Biotechnology (Dallas, TX). Affinity-purified rabbit polyclonal anti-Cx46 intracellular loop and anti-Cx50 C-terminus antibodies have been previously described [3,15]. Horseradish peroxidase–conjugated goat AffiniPure anti-rabbit immunoglobulin G (IgG; H+L; 111–035–144; lot # 123520 and 135724) and horseradish peroxidase–conjugated goat AffiniPure $F(ab')_2$ fragment goat anti-mouse IgG, $F(ab')_2$ fragment-specific (115–036–072; lot # 111686 and 135721) antibodies were obtained from Jackson ImmunoResearch (West Grove, PA).

Animals: Cx50D47A (*No2*, ENU-326) mice (originally identified by Favor by screening for the cataract phenotype following ethylnitrosourea (ENU-326) mutagenesis [4]) were maintained as previously described [3]. Wild-type C57BL/6J mice (# 000664) and homozygous *Chop* knockout mice (# 005530) were obtained from the Jackson Laboratory (Genetic Resource Science at the Jackson Laboratory. 2008. Expression/Specificity Patterns of Cre Alleles, 2008 Direct Data Submission from Genetic Resource Science: MGI: J:137887). Lenses from some of these mice (on a C57BL/6J background) were examined between 7 and 8 months of age. The *Chop* knockout mice were bred into the C3H line for six generations before performing the experiments. Heterozygous *Chop* knockout ($Chop^{+/-}$) mice were mated with homozygous Cx50D47A ($Cx50^{D47A/D47A}$) mice to generate heterozygous *Chop* knockout mice that were homozygous for the Cx50 mutation ($Chop^{+/-}$-$Cx50^{D47A/D47A}$). Mice of this genotype from different litters were mated to obtain homozygous Cx50D47A mice that were wild type for *Chop* or heterozygous or homozygous for the *Chop* deletion. All the animal procedures followed the University of Chicago Animal Care and Use Committee guidelines and were conducted in accordance with the Association for Research in Vision and Ophthalmology (ARVO) Statement for the Use of Animals in Ophthalmic and Vision Research and National Institutes of Health (NIH) regulations.

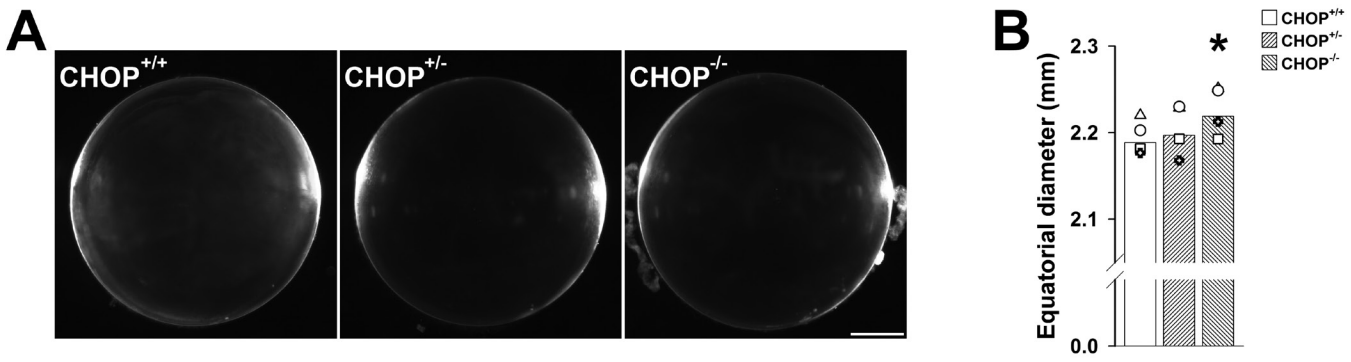

Figure 1. Deletion of *Chop* does not affect lens transparency. **A**: Dark-field photomicrographs of lenses from wild-type *Chop* (*Chop*$^{+/+}$) and heterozygous (*Chop*$^{+/-}$) and homozygous (*Chop*$^{-/-}$) *Chop* knockout mice at 1 month of age. Scale bar: 474 µm. **B**: Graph showing the equatorial diameters determined from dark-field photomicrographs of lenses from wild-type *Chop* (*Chop*$^{+/+}$) and heterozygous (*Chop*$^{+/-}$) and homozygous (*Chop*$^{-/-}$) *Chop* knockout mice (n = 4 biological replicates). The data points are presented with different symbols, each indicating a different set (containing all three genotypes) of lenses from littermate mice. Bars represent the mean. The asterisk denotes significant differences from *Chop*$^{+/+}$ ($p<0.05$).

Quantification of lens opacity and lens size: Dark-field photomicrographs of lenses from 1-month-old mouse littermates containing all the genotypes (referred to as a set) were obtained using a Zeiss Stemi-2000C dissecting scope (Carl Zeiss, München, Germany). The same settings (i.e., magnification, illumination, and exposure time) were used to photograph all lenses in each set. Cataracts (opacities) were quantified in photomicrographs by integrating the gray values over a circular region of interest using NIH ImageJ software, as previously performed [16]. The circular region used to analyze all images was identical in size. These data are reported in arbitrary units. The dimensions of the equatorial diameters were determined from the photomicrographs using NIH ImageJ software. The opacities and the diameters were measured in both lenses of each mouse (unless one of the lenses was damaged during dissection); the reported values are the averages of the measurements of the two lenses for each mouse.

Real-time quantitative PCR: Real-time quantitative PCR (RT-qPCR) was performed similarly to our previous study [6]. Lenses from 1-month-old homozygous Cx50D47A mouse littermates of different *Chop* genotypes were homogenized in QIAzol Lysis Reagent (Qiagen, Valencia, CA) using a glass–glass homogenizer, and the RNA was purified using the miRNeasy Mini Kit (Qiagen). The concentrations of RNA were determined using a NanoDrop spectrophotometer (Thermo Fisher Scientific) and the quality of the RNA was analyzed on an Agilent Bio-Analyzer (Agilent Technologies, Santa Clara, CA). cDNA was synthesized using the QuantiTect Reverse Transcription Kit (Qiagen). RT-qPCR was performed on a 7500 Fast Real-time PCR System (Applied Biosystems, Foster City, CA) using a cDNA aliquot, a primer set for the RNA of interest, and Fast SYBR® Green Master Mix (Life Technologies, Grand Island, NY). The primer sequences are listed in Table 1. These primer sets had efficiencies within a 95% confidence interval, and they did not produce primer dimers as assessed by the melting curves. All reaction mixes contained equal amounts of RNA. Each sample was run in triplicate (i.e., technical replicates) for each primer set. Each variable was studied using at least three independent sets of littermates (i.e., biological replicates). The transcript for cyclophilin A was used as the internal control to normalize the relative levels of RNA among the different genotypes. The spliced/total *Xbp-1* (s*Xbp-1*/t*Xbp-1*) ratio was calculated by dividing the $2^{-\Delta CT}$ of spliced *Xbp-1* by the $2^{-\Delta CT}$ of total *Xbp-1*, where $\Delta C_T = C_T$ for spliced or total *Xbp-1* in the sample – C_T for *cyclophilin A* in that sample. Graphs were prepared using SigmaPlot 10.0 (Systat Software, Inc., San Jose, CA).

Immunoblotting: Whole-lens homogenates from 1-month-old homozygous Cx50D47A mice that were *Chop* wild-type or heterozygous or homozygous *Chop* knockout were prepared by homogenizing the two lenses from each mouse in PBS containing 4 mM EDTA, 2 mM phenylmethylsulfonyl fluoride, 20 mM NaF, 10 mM Na_3VO_4, pH 7.4 and cOmplete Mini EDTA-free Protease Inhibitor Cocktail (Roche Applied Science, Indianapolis, IN) using a glass–glass homogenizer followed by sonication. Protein concentrations were determined using the Bio-Rad Protein Assay Dye Reagent Concentrate (Bio-Rad) based on the Bradford method [17]. Aliquots from lens homogenates containing equal amounts of total protein were loaded in each lane and resolved by

sodium dodecyl sulfate–polyacrylamide gel electrophoresis (SDS–PAGE). The gels were then blotted onto Immobilon P membranes (Millipore, Bedford, MA) using a wet transfer apparatus. Then, the membranes were stained with Ponceau S (to verify equal electrotransfer of the proteins) before being subjected to immunoblotting as previously described [6,18]. The X-ray films were scanned on a flat-bed scanner (Epson Perfection V700 Photo; Epson America, Long Beach, CA) to obtain a digital image for quantification of the bands. The bands obtained in at least three independent experiments (i.e., biological replicates) were quantified by densitometry using a rectangular box that encompassed the immunoreactive band(s) using Adobe Photoshop CS3 (Adobe Systems Inc., San Jose, CA). The box size used to quantify the immunoreactive band was kept constant for each set of littermates containing all three genotypes. The same size box was used to obtain a background value in each lane and correct the integrated band density (Photoshop Extended: Evaluation of gel images; Photoshop Extended: Performing a comparative analysis of bands; Using Photoshop CC to quantify band intensity in a DNA gel). The results are reported in arbitrary units. Graphs were prepared using SigmaPlot 10.0 (Systat Software, Inc.).

Statistical analysis: The raw data obtained from heterozygotes and homozygotes were compared to the raw data obtained from wild-type (or control) littermates to assess statistical significance using the Student *t*-test. A p value <0.05 was considered significant. The number of sets of littermates containing all genotypes (statistical "n") was at least three for each type of data presented.

RESULTS

Deletion of Chop did not affect the lens transparency of wild-type mice: Germline deletion of *Chop* has been reported to induce no major phenotypic effects on mouse organs, although histomorphometric analysis showed a decreased bone formation rate at 1–12 months of age [19-21]. However, the lens was not specifically examined in these studies. To test whether expression of *Chop* was required for lens transparency in normal mice, we studied the lenses from heterozygous and homozygous *Chop* null mice and compared them with those of wild-type animals. Microscopic examination under dark-field illumination showed that the lenses from 1-month-old heterozygous and homozygous *Chop* null mice were transparent and appeared indistinguishable from those of their wild-type littermates (Figure 1A). At 2 months of age, lenses from wild-type and *Chop* null heterozygous and homozygous littermates were almost completely transparent and appeared identical, but they had a few of the typical

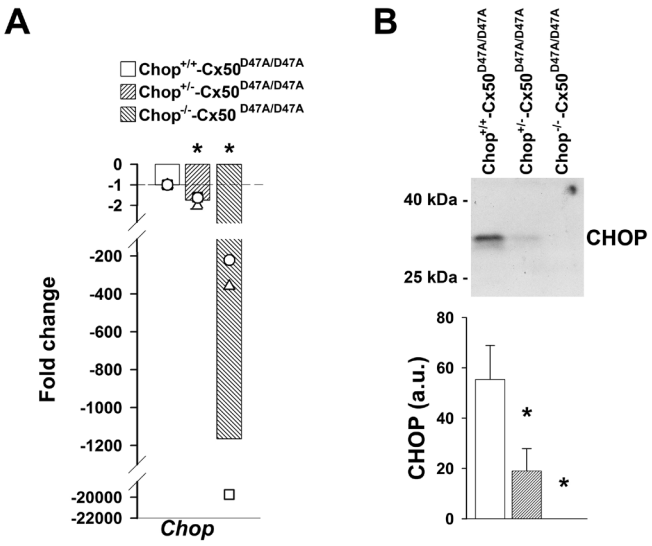

Figure 2. *Chop* deletion was confirmed. **A**: Graph shows the fold change of *Chop* transcript levels in lenses from 1-month-old homozygous Cx50D47A mice that were *Chop*$^{+/-}$ and *Chop*$^{-/-}$ relative to levels of *Chop*$^{+/+}$ (*Chop*$^{+/+}$-Cx50$^{D47A/D47A}$) lenses as determined by real-time quantitative PCR. The values obtained in each of three independent biological replicates are shown with different symbols representing each set of littermates. The bars represent the geometric mean of the fold change obtained in the biological replicates. The value obtained in *Chop*$^{+/+}$-Cx50$^{D47A/D47A}$ mice was considered as the reference (short dashed line at fold change = −1). **B**: Immunoblot of CCAAT/enhancer-binding homologous protein (CHOP) in homogenates from lenses of 1-month-old homozygous Cx50D47A littermates that were *Chop*$^{+/+}$, *Chop*$^{+/-}$, and *Chop*$^{-/-}$. The migration positions of the molecular mass markers are indicated on the left. Graph shows the mean (bar) + standard error of the mean of the densitometric values of the immunoreactive bands obtained from three biological replicates expressed in arbitrary units (a.u.). Asterisks denote significant differences from *Chop*$^{+/+}$-Cx50$^{D47A/D47A}$ values ($p<0.05$).

micro-opacities of this mouse line (not shown). Moreover, wild-type and homozygous *Chop* null lenses from mice of the C57BL/6J background appeared similar and mostly transparent at >7 months of age (not shown).

We found a small variation in the equatorial diameters of wild-type lenses from different litters (Figure 1B). Similar variations were found in the lens diameters of heterozygous and homozygous *Chop* knockout mice. However, we consistently found that the equatorial diameters of homozygous *Chop* null lenses were slightly larger (1.7%) than those of their wild-type littermates, while the lens diameters from heterozygous *Chop* knockout mice were not significantly different from those of the wild-type littermates (Figure 1B). There were no detectable differences in lens weights.

Deletion of Chop did not improve lens transparency or size in Cx50D47A mice: To elucidate whether increased CHOP

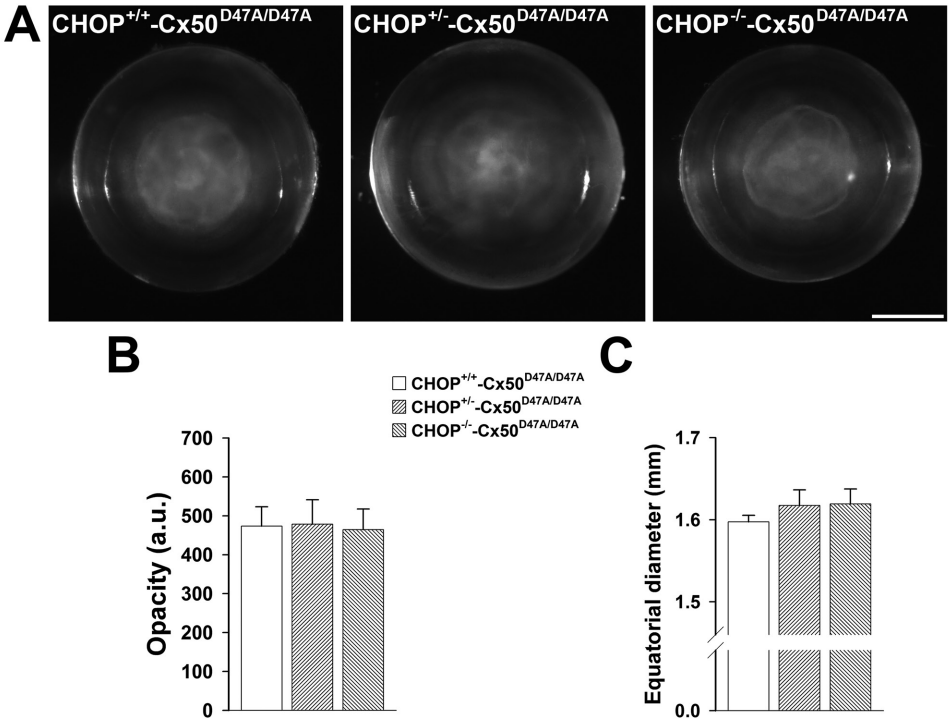

Figure 3. Deletion of *Chop* does not affect the extent of opacity or size of Cx50$^{D47A/D47A}$ lenses. **A**: Dark-field photomicrographs of lenses from 1-month-old homozygous Cx50D47A mice that were wild type for *Chop* (*Chop*$^{+/+}$) or heterozygous (*Chop*$^{+/-}$) or homozygous (*Chop*$^{-/-}$) *Chop*-null. Scale bar: 489 µm. **B**: Graph showing the quantification of the cataract (opacity) in arbitrary units (a.u.). Data are presented as the mean (bar) + standard error of the mean (SEM). **C**: Graph showing the equatorial diameters determined from dark-field photomicrographs of lenses from homozygous Cx50D47A mice that were wild type for *Chop* (*Chop*$^{+/+}$) or heterozygous (*Chop*$^{+/-}$) or homozygous (*Chop*$^{-/-}$) knockout for *Chop*. Data are presented as the mean (bar) + SEM. For the calculations in **B** and **C**, n = 4 sets of littermates containing all three genotypes.

played a unique role for the cataract phenotype of homozygous Cx50D47A lenses, we generated and studied litters of mice that were homozygous for the Cx50D47A mutation and contained all three *Chop* genotypes (wild-type and heterozygous and homozygous *Chop* knockout). These animals were tested for the expression of *Chop* (Figure 2A). The levels of *Chop* mRNA decreased to about half in *Chop*$^{+/-}$-Cx50$^{D47A/D47A}$ lenses as compared with the values in *Chop*$^{+/+}$-Cx50$^{D47A/D47A}$ lenses (Figure 2A; $p<0.05$). RT-qPCR revealed that *Chop* mRNA was reduced by 1,164 times on average in *Chop*$^{-/-}$-Cx50$^{D47A/D47A}$ lenses (Figure 2A; $p<0.05$). These results are consistent with the absence of *Chop* expression in *Chop*$^{-/-}$-Cx50$^{D47A/D47A}$ samples and confirm the deletion of *Chop* in knockout animals, as previously reported [21]. Levels of CHOP protein were weakly detectable in *Chop*$^{+/-}$-Cx50$^{D47A/D47A}$ lenses, and they were undetectable in *Chop*$^{-/-}$-Cx50$^{D47A/D47A}$ lenses (Figure 2B).

Having verified the expected reductions of *Chop* RNA and protein, we examined the lenses of these mice under dark-field illumination. All lenses contained cataracts, regardless of the *Chop* genotype (Figure 3A). Quantitation of the lens images using ImageJ showed that there were no significant differences in lens opacities, nor did the equatorial lens diameters differ between littermates of Cx50$^{D47A/D47A}$ mice with different *Chop* genotypes (Figure 3B,C).

Deletion of Chop did not affect the activation of the PERK-dependent pathway in Cx50D47A lenses: We previously showed a significant increase in the phosphorylated form of EIF2α (P-EIF2α) in homozygous Cx50D47A lenses. In these lenses, the P-EIF2α/EIF2α ratio was 3.3 times the value in wild-type lenses [6]. Because *Chop* deletion in mouse models of other diseases alters phosphorylation of EIF2α [22,23], we tested whether deletion of *Chop* affected the levels of P-EIF2α or the P-EIF2α/EIF2α ratio. The P-EIF2α levels and P-EIF2α/EIF2α ratio in lenses from *Chop*$^{+/-}$-Cx50$^{D47A/D47A}$ and *Chop*$^{-/-}$-Cx50$^{D47A/D47A}$ mice did not significantly differ from those in *Chop*$^{+/+}$-Cx50$^{D47A/D47A}$ animals as detected by immunoblotting (Figure 4A).

Deletion of *Chop* could also affect other aspects of the ER response to unfolded proteins. For example, *Chop* deletion decreases the spliced form of X-box-binding protein 1 (XBP-1) in the retina of T7M rhodopsin mice [23], but it does not affect *Xbp-1* splicing induced in retinal ganglion cells after optic nerve crush [24]. To test whether the deletion of *Chop* affected *Xbp-1* splicing in lenses of homozygous Cx50D47A mice, we used RT-qPCR to quantify the ratio of spliced versus total *Xbp-1* mRNA (s*Xbp-1*/t*Xbp-1*). We found that the s*Xbp-1*/t*Xbp-1* ratio was not significantly different in lenses from *Chop*$^{+/-}$-Cx50$^{D47A/D47A}$, *Chop*$^{-/-}$-Cx50$^{D47A/D47A}$, and *Chop*$^{+/+}$-Cx50$^{D47A/D47A}$ littermates (Figure 4B).

Levels of lens fiber connexins were not altered by Chop deletion in Cx50D47A mice: Among other roles, CHOP is a key regulator of autophagy [25-27], a pathway implicated in the degradation of connexins [28]. We previously showed that homozygous Cx50D47A mice have decreased levels of the lens fiber cell connexins, Cx46 and Cx50 (27.7% and 3.1% of the wild-type values, respectively, at 3 weeks of age) [29], likely resulting from degradation of the proteins. To determine the effect of *Chop* deletion on levels of Cx46 and Cx50, we performed immunoblots for Cx46 and Cx50 on whole-lens homogenates of *Chop*$^{+/+}$-Cx50$^{D47A/D47A}$, *Chop*$^{+/-}$-Cx50$^{D47A/D47A}$, and *Chop*$^{-/-}$-Cx50$^{D47A/D47A}$ mice. Levels of these connexins were not significantly different among littermates of the different *Chop* genotypes (Figure 5).

Deletion of Chop did not affect the increased expression of Irs2 and Trib3 in Cx50D47A lenses: We previously showed that the mRNA levels of *Irs2* and *Trib3* are increased by 7.3-fold (range: 3.7–14.4) and 1,002-fold (range: 299–1,873) in homozygous Cx50D47A lenses compared with wild-type lenses [6]. Because these transcripts were identified as prosurvival genes in early stage erythroblasts [30], we hypothesized that this increase depended on the increase in CHOP or represented a compensatory response to it. To test this hypothesis, we performed RT-qPCR on lens RNA from *Chop*$^{+/+}$-Cx50$^{D47A/D47A}$, *Chop*$^{+/-}$-Cx50$^{D47A/D47A}$, and *Chop*$^{-/-}$-Cx50$^{D47A/D47A}$ mouse littermates. Average levels of *Irs2* decreased by 1.4-fold in *Chop*$^{+/-}$-Cx50$^{D47A/D47A}$ lenses and increased by 1.2-fold in *Chop*$^{-/-}$-Cx50$^{D47A/D47A}$ lenses (Figure 6A). Average levels of *Trib3* increased by 1.2-fold in *Chop*$^{+/-}$-Cx50$^{D47A/D47A}$ lenses and decreased by 1.5-fold in *Chop*$^{-/-}$-Cx50$^{D47A/D47A}$ lenses (Figure 6B). These differences were not statistically significant compared with *Chop*$^{+/+}$-Cx50$^{D47A/D47A}$ lenses, and they did not represent a substantial return toward the levels previously observed in wild-type mice (*Chop*$^{+/+}$-Cx50$^{+/+}$).

Deletion of Chop in Cx50D47A mice did not alter the levels of lens proteins from different subcellular compartments:

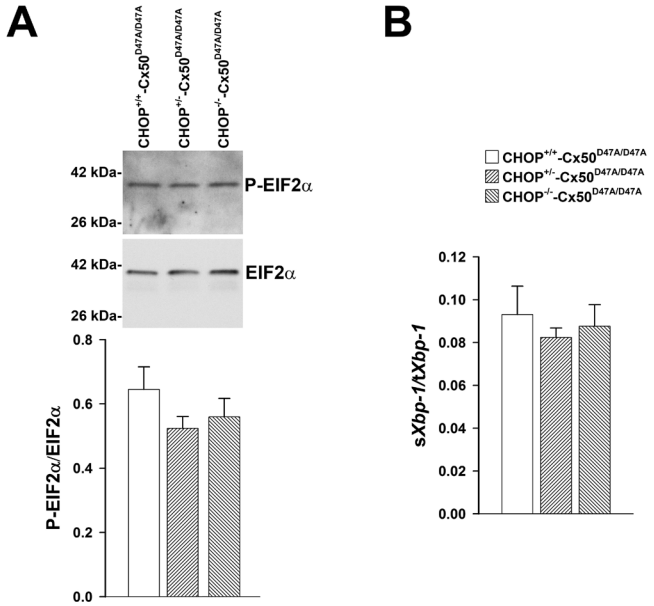

Figure 4. Deletion of *Chop* in Cx50D47A homozygotes does not affect activation of endoplasmic reticulum (ER) stress transduction pathways. **A**: Immunoblots of immunoreactive phosphorylated (top panel) and total (middle panel) eukaryotic translation initiation factor-2A (P-EIF2α and EIF2α, respectively) in total lens homogenates from 1-month-old homozygous Cx50D47A mice that were wild type for *Chop* or heterozygous or homozygous *Chop* knockout. The migration positions of the molecular mass markers are indicated on the left. The graph in the bottom panel shows the ratios of phosphorylated to total EIF2α (P-EIF2α/EIF2α) calculated from the densitometric values of the immunoreactive bands obtained from three independent biological replicates as the mean (bar) + standard error of the mean (SEM). **B**: Graph showing the ratio of spliced (s*Xbp-1*) to total (t*Xbp-1*) *Xbp-1* in lenses from 1-month-old homozygous Cx50D47A mouse littermates that were wild type for *Chop* (*Chop*$^{+/+}$) or heterozygous (*Chop*$^{+/-}$) or homozygous (*Chop*$^{-/-}$) *Chop* knockout as determined by real-time quantitative PCR in three independent biological replicates. Data are presented as the mean (bar) + SEM.

Because CHOP has been implicated in modulating differentiation in other tissues [12], and expression of Cx50D47A impairs lens cell differentiation with retention of organelles in fiber cells [3], we investigated whether deletion of *Chop* altered levels of proteins from different subcellular compartments that are increased in homozygous Cx50D47A lenses. In these lenses, histone H3 (a chromatin component) is increased more than 10-fold, TOM20 (a mitochondrial protein) is increased nearly 3-fold, and calreticulin (a protein that binds calcium and is mainly localized in the ER) is increased 2.6-fold as compared with levels in wild-type lenses [3,6]. Immunoblots of lens homogenates from Cx50$^{D47A/D47A}$ littermates that were wild type for *Chop* or heterozygous or homozygous for the deletion of *Chop* showed that levels of histone

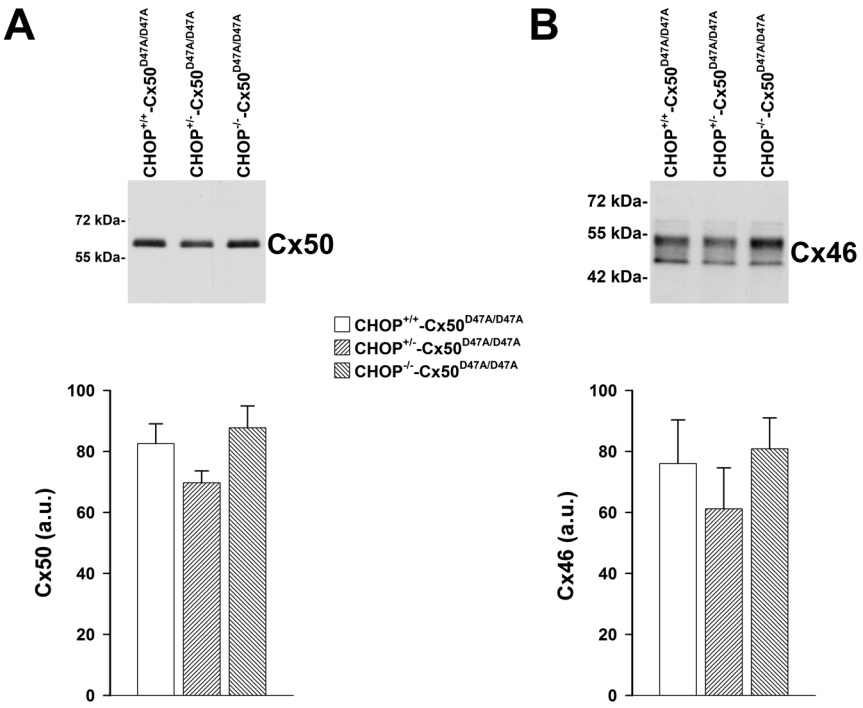

Figure 5. Deletion of *Chop* in $Cx50^{D47A/D47A}$ mice does not alter levels of lens fiber connexins. **A**, **B**: Immunoblots of connexin50 (Cx50; **A**, top) and connexin46 (Cx46; **B**, top) in lens homogenates prepared from 1-month-old $Cx50^{D47A/D47A}$ mice that were wild type for *Chop* ($Chop^{+/+}$) or heterozygous ($Chop^{+/-}$) or homozygous ($Chop^{-/-}$) *Chop* knockout. The migration positions of the molecular mass markers are indicated on the left. Graphs at the bottom show the quantification of the density of the Cx50 (**A**) and Cx46 (**B**) immunoreactive bands. Data are presented as the mean (bar) + standard error of the mean (n = 5 sets for Cx50; n = 3 sets for Cx46).

H3, TOM20, and calreticulin were not significantly different (Figure 7).

Cebpb is increased in Cx50D47A lenses, but decreased by Chop deletion: CCAAT/enhancer-binding protein β (CEBPβ) is a major dimerization partner of CHOP that contributes to transcriptional regulation and is involved in several processes, including proliferation, differentiation, and cell death. We found that *Cebpb* mRNA was significantly increased (by ~6.4-fold) in $Chop^{+/+}$-$Cx50^{D47A/D47A}$ lenses relative to its levels in wild-type mice (Figure 8A). Homozygous (but not heterozygous) deletion of *Chop* resulted in a significant decrease (by ~4.3-fold) in *Cebpb* mRNA levels in homozygous Cx50D47A lenses (Figure 8B). This change would return *Cebpb* transcripts close to wild-type levels.

DISCUSSION

Our results demonstrate that expression of *Chop* is dispensable for the maintenance of transparency in wild-type lenses, since we found that lenses of mice in which only *Chop* was deleted did not exhibit increased opacities. This finding agrees with the initial report on the *Chop* knockout mouse line describing the absence of gross abnormalities when the animals are maintained on a regular diet [19-21]. However, deletion of *Chop* slightly increased lens size, implying that CHOP contributes directly or indirectly to the regulation of lens size in the normal animal. CHOP has previously been

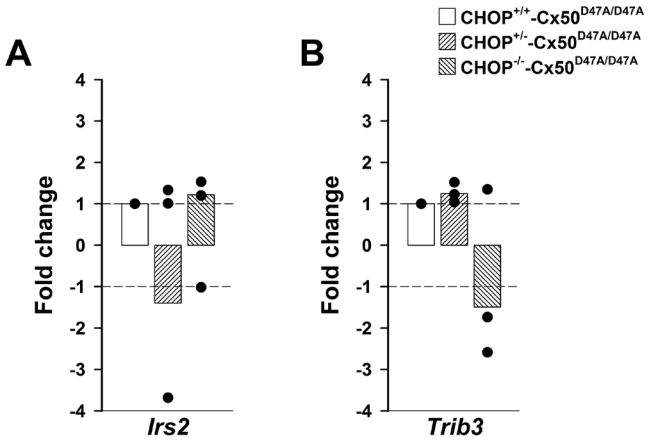

Figure 6. Deletion of *Chop* in $Cx50^{D47A/D47A}$ mice does not alter *Irs2* or *Trib3* expression. **A**, **B**: Graphs show the fold change of *Irs2* (**A**) and *Trib3* (**B**) mRNAs in 1-month-old homozygous Cx50D47A lenses that were heterozygous ($Chop^{+/-}$-$Cx50^{D47A/D47A}$) and homozygous ($Chop^{-/-}$-$Cx50^{D47A/D47A}$) for the *Chop* deletion relative to the levels in wild-type ($Chop^{+/+}$-$Cx50^{D47A/D47A}$) littermates as determined by real-time quantitative PCR. The bars represent the geometric mean of the fold change obtained in three independent experiments (black circles) using the value obtained in $Chop^{+/+}$-$Cx50^{D47A/D47A}$ littermates as the reference (short dashed lines at fold change = +1 and −1).

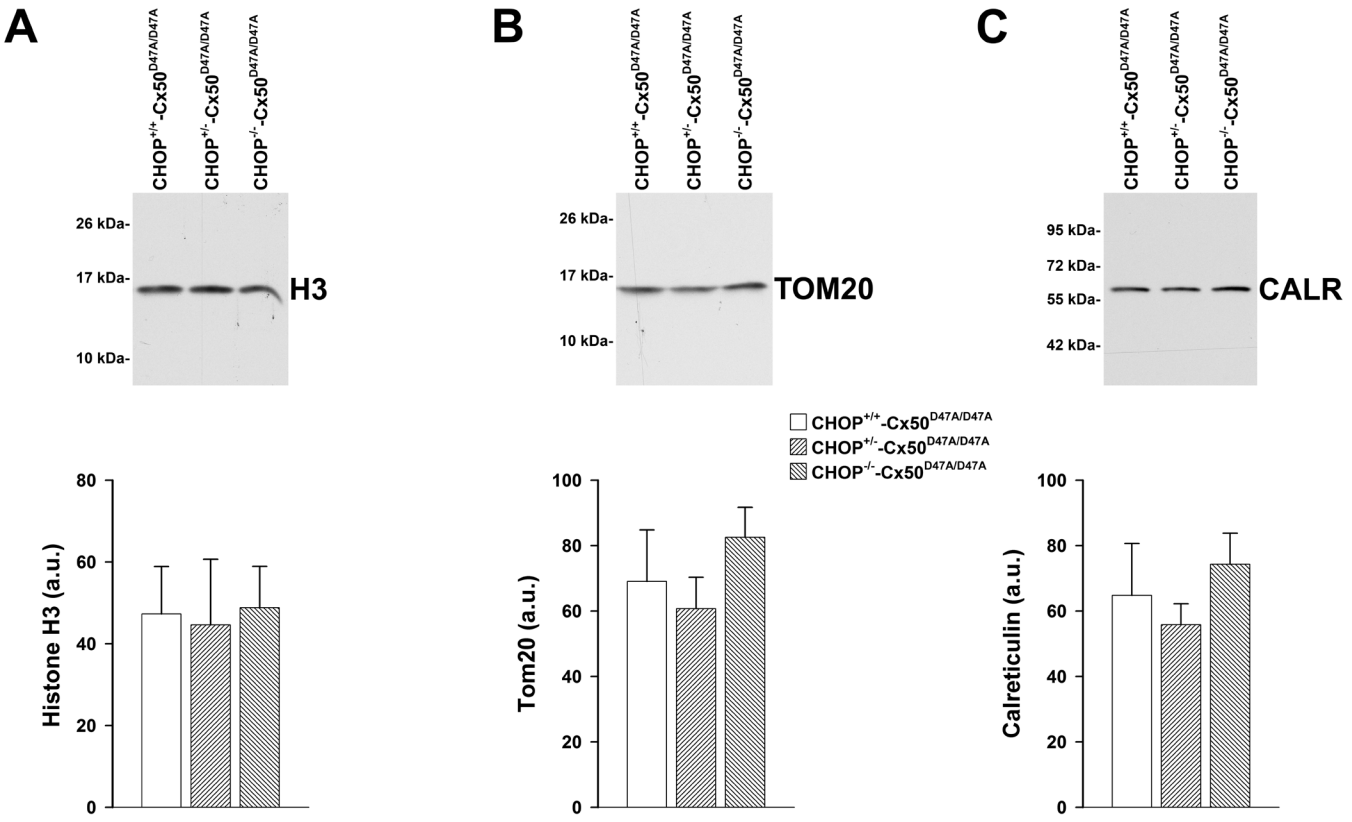

Figure 7. Deletion of *Chop* does not affect levels of proteins associated with different intracellular compartments that are not completely removed during cell differentiation in Cx50D47A lenses. **A**–**C**: Immunoblots of histone H3 (H3; **A**, top panel), translocase of outer mitochondrial membrane 20 (TOM20; **B**, top panel) and calreticulin (CALR; **C**, top panel) in lens homogenates prepared from 1-month-old Cx50D47A homozygotes that were wild type for *Chop* (*Chop*$^{+/+}$) or heterozygous (*Chop*$^{+/-}$) or homozygous (*Chop*$^{-/-}$) *Chop* knockout. The migration positions of the molecular mass markers are indicated on the left. Graphs in the bottom panels show the densitometric quantification of the H3 (**A**), TOM20 (**B**), and CALR (**C**) immunoreactive bands. Data are presented as the mean (bar) + standard error of the mean obtained in three independent biological replicates.

implicated in increased general body size, since female mice given a regular or a high-fat diet increase in body weight and fat mass [31]. The increase in lens size in our mice is unlikely to result from increased fat mass, since the animals were maintained on a regular diet and there is no fat mass associated with the lens. Rather, it is more likely that the slight increase in lens size results from disrupting other CHOP roles (such as cell death or promotion of oxidizing conditions in the ER) [21,32].

We also found that deletion of *Chop* did not significantly improve the opacities of homozygous Cx50D47A mice. Thus, although *Chop* mRNA levels are significantly increased in these mice, this transcript is not the critical factor leading to cataract formation and progression. We speculate that deletion of *Chop* would also have little or no effect in animals with cataracts caused by different etiologies, including mutations of other major lens proteins like αA-crystallin and Aquaporin0 [9,10], where increased levels of *Chop* mRNA and CHOP protein are also found. While deletion of *Chop* ameliorates the effects induced by stresses in some systems, it is ineffective at mitigating the pathology in others. In *Chop*$^{-/-}$ mice, survival of retinal ganglion cells following optic nerve crush is increased as compared with wild-type mice [24]. Deletion of *Chop* delays the onset of diabetes in a mouse model of type 2 diabetes [26]. It also decreases the cardiac hypertrophy, fibrosis, and myocardial dysfunction induced by transverse aortic occlusion [22]. In contrast, deletion of *Chop* accentuates skeletal muscle atrophy in a mouse model of spinal and bulbar muscular atrophy [27]. In addition, *Chop* deletion does not rescue photoreceptors and worsens the pathology in a mouse model of autosomal dominant retinitis pigmentosa [23].

Our results imply that the Cx50 mutation has a strong effect on several parameters that cannot be overcome by

deletion of *Chop*. Homozygous Cx50D47A mice have extremely small lenses [3]. Although this may have resulted from increased cell death, deletion of *Chop* (an inducer of cell death in other systems) in homozygous Cx50D47A mice did not increase lens size. In addition, *Chop* deletion did not increase the levels of lens Cx46 or Cx50, decrease transcript levels of *Trib3* or *Irs2*, improve differentiation (degradation of nuclei and mitochondria), or ameliorate the cataract phenotype.

Of all the parameters studied, a decrease in the levels of *Cebpb* transcripts was the only significant change detected in homozygous Cx50D47A lenses after homozygous deletion of *Chop*. This result implies that, in the lens, *Cebpb* is either a direct or indirect target of CHOP. Because mouse CEBPβ can autoregulate its transcription, it is possible that the lack of CHOP (one of the CEBPβ dimerizing partners) led to a decrease in CEBPβ levels, leading to an attenuation of derepression of its transcription [33]. In contrast, in the livers of lipopolysaccharide-treated rats, CEBPβ increases transcription of *Chop* [34], implying that *Chop* is a target of CEBPβ.

The lack of a major effect of deletion of *Chop* on the phenotype and several of the parameters studied in homozygous Cx50D47A lenses may be due to alterations in the expression of other transcription factor(s) that compensate for the absence of CHOP. In addition, the effects of CHOP in homozygous Cx50D47A lenses may have been diminished by αB-crystallin, which is stress responsive [35-38] and has increased levels in these lenses [3]. This crystallin has been implicated in attenuating the response of different cell types to strong cellular stresses [39,40]. αB-crystallin can bind to partially processed caspase-3 and inhibit its autocatalytic activation [41].

Taken together, our results suggest that CHOP influences some aspects of the diseased lens (like lens *Cebpb* transcript levels), but it is not a unique critical etiological factor for the cataracts and impaired differentiation of Cx50D47A lenses.

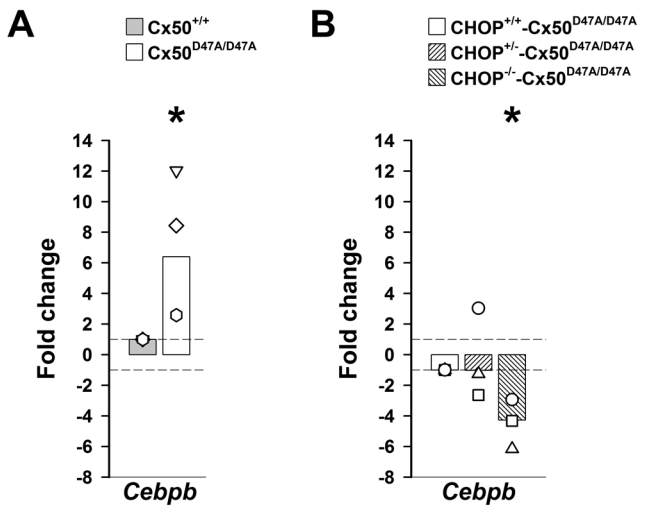

Figure 8. *Cebpb* expression is increased in Cx50$^{D47A/D47A}$ lenses, and deletion of *Chop* in Cx50$^{D47A/D47A}$ mice reduces this increase. **A**: Graph showing the fold change of transcript levels for *Cebpb* as determined by real-time quantitative PCR (RT-qPCR) in 1-month-old homozygous Cx50D47A lenses relative to those in their wild-type littermates. **B**: Graph showing the fold change of transcript levels for *Cebpb* as determined by RT-qPCR in 1-month-old lenses from homozygous Cx50D47A mice that were heterozygous (*Chop*$^{+/-}$-Cx50$^{D47A/D47A}$) and homozygous (*Chop*$^{-/-}$-Cx50$^{D47A/D47A}$) *Chop* knockout relative to the levels in lenses from their littermates that were wild type for *Chop* (*Chop*$^{+/+}$-Cx50$^{D47A/D47A}$). The values obtained in each of three independent biological replicates are shown in different symbols (each representing a different set of mouse littermates containing all genotypes). The bars represent the geometric mean of the fold change obtained in the biological replicates. The value obtained in Cx50$^{+/+}$ littermates was considered as the reference in panel **A**, and the value obtained in *Chop*$^{+/+}$-Cx50$^{D47A/D47A}$ littermates was considered as the reference in panel **B** (short dashed lines at fold change = +1 and −1). Asterisks indicate a significant difference ($p<0.05$) from the values in the wild type (in panel **A**) and *Chop*$^{+/+}$-Cx50$^{D47A/D47A}$ (in panel **B**).

ACKNOWLEDGMENTS

This work was supported by National Institutes of Health Grant R01EY08368 (ECB).

REFERENCES

1. Reddy MA, Francis PJ, Berry V, Bhattacharya SS, Moore AT. Molecular genetic basis of inherited cataract and associated phenotypes. Surv Ophthalmol 2004; 49:300-15. [PMID: 15110667].

2. Shiels A, Bennett TM, Hejtmancik JF. Cat-Map: putting cataract on the map. Mol Vis 2010; 16:2007-15. [PMID: 21042563].

3. Berthoud VM, Minogue PJ, Yu H, Schroeder R, Snabb JI, Beyer EC. Connexin50D47A decreases levels of fiber cell connexins and impairs lens fiber cell differentiation. Invest Ophthalmol Vis Sci 2013; 54:7614-22. [PMID: 24204043].

4. Favor J. A comparison of the dominant cataract and recessive specific-locus mutation rates induced by treatment of male mice with ethylnitrosourea. Mutat Res 1983; 110:367-82. [PMID: 6877261].

5. Steele EC Jr, Lyon MF, Favor J, Guillot PV, Boyd Y, Church RL. A mutation in the connexin 50 (Cx50) gene is a candidate for the *No2* mouse cataract. Curr Eye Res 1998; 17:883-9. [PMID: 9746435].

6. Berthoud VM, Minogue PJ, Lambert PA, Snabb JI, Beyer EC. The cataract-linked mutant connexin50D47A causes

endoplasmic reticulum stress in mouse lenses. J Biol Chem 2016; 291:17569-78. [PMID: 27317663].

7. Firtina Z, Danysh BP, Bai X, Gould DB, Kobayashi T, Duncan MK. Abnormal expression of collagen IV in lens activates unfolded protein response resulting in cataract. J Biol Chem 2009; 284:35872-84. [PMID: 19858219].

8. Palsamy P, Bidasee KR, Shinohara T. Selenite cataracts: activation of endoplasmic reticulum stress and loss of Nrf2/Keap1-dependent stress protection. Biochim Biophys Acta 2014; 1842:1794-805. [PMID: 24997453].

9. Watson GW, Andley UP. Activation of the unfolded protein response by a cataract-associated αA-crystallin mutation. Biochem Biophys Res Commun 2010; 401:192-6. [PMID: 20833134].

10. Zhou Y, Bennett TM, Shiels A. Lens ER-stress response during cataract development in *Mip*-mutant mice. Biochim Biophys Acta 2016; 1862:1433-42. [PMID: 27155571].

11. Oyadomari S, Mori M. Roles of CHOP/GADD153 in endoplasmic reticulum stress. Cell Death Differ 2004; 11:381-9. [PMID: 14685163].

12. Yang Y, Liu L, Naik I, Braunstein Z, Zhong J, Ren B. Transcription factor C/EBP homologous protein in health and diseases. Front Immunol 2017; 8:1612-[PMID: 29230213].

13. Ron D, Habener JF. CHOP, a novel developmentally regulated nuclear protein that dimerizes with transcription factors C/EBP and LAP and functions as a dominant-negative inhibitor of gene transcription. Genes Dev 1992; 6:439-53. [PMID: 1547942].

14. Ramji DP, Foka P. CCAAT/enhancer-binding proteins: structure, function and regulation. Biochem J 2002; 365:561-75. [PMID: 12006103].

15. Berthoud VM, Minogue PJ, Guo J, Williamson EK, Xu X, Ebihara L, Beyer EC. Loss of function and impaired degradation of a cataract-associated mutant connexin50. Eur J Cell Biol 2003; 82:209-21. [PMID: 12800976].

16. Jara O, Minogue PJ, Berthoud VM, Beyer EC. Chemical chaperone treatment improves levels and distributions of connexins in Cx50D47A mouse lenses. Exp Eye Res 2018; 175:192-8. [PMID: 29913165].

17. Bradford MM. A rapid and sensitive method for the quantitation of microgram quantities of protein utilizing the principle of protein-dye binding. Anal Biochem 1976; 72:248-54. [PMID: 942051].

18. Minogue PJ, Tong JJ, Arora A, Russell-Eggitt I, Hunt DM, Moore AT, Ebihara L, Beyer EC, Berthoud VM. A mutant connexin50 with enhanced hemichannel function leads to cell death. Invest Ophthalmol Vis Sci 2009; 50:5837-45. [PMID: 19684000].

19. Oyadomari S, Takeda K, Takiguchi M, Gotoh T, Matsumoto M, Wada I, Akira S, Araki E, Mori M. Nitric oxide-induced apoptosis in pancreatic β cells is mediated by the endoplasmic reticulum stress pathway. Proc Natl Acad Sci USA 2001; 98:10845-50. [PMID: 11526215].

20. Pereira RC, Stadmeyer L, Marciniak SJ, Ron D, Canalis E. C/EBP homologous protein is necessary for normal osteoblastic function. J Cell Biochem 2006; 97:633-40. [PMID: 16220546].

21. Zinszner H, Kuroda M, Wang X, Batchvarova N, Lightfoot RT, Remotti H, Stevens JL, Ron D. CHOP is implicated in programmed cell death in response to impaired function of the endoplasmic reticulum. Genes Dev 1998; 12:982-95. [PMID: 9531536].

22. Fu HY, Okada K, Liao Y, Tsukamoto O, Isomura T, Asai M, Sawada T, Okuda K, Asano Y, Sanada S, Asanuma H, Asakura M, Takashima S, Komuro I, Kitakaze M, Minamino T. Ablation of C/EBP homologous protein attenuates endoplasmic reticulum-mediated apoptosis and cardiac dysfunction induced by pressure overload. Circulation 2010; 122:361-9. [PMID: 20625112].

23. Nashine S, Bhootada Y, Lewin AS, Gorbatyuk M. Ablation of C/EBP homologous protein does not protect T17M *RHO* mice from retinal degeneration. PLoS One 2013; 8:e63205-[PMID: 23646198].

24. Hu Y, Park KK, Yang L, Wei X, Yang Q, Cho KS, Thielen P, Lee AH, Cartoni R, Glimcher LH, Chen DF, He Z. Differential effects of unfolded protein response pathways on axon injury-induced death of retinal ganglion cells. Neuron 2012; 73:445-52. [PMID: 22325198].

25. B'chir W, Chaveroux C, Carraro V, Averous J, Maurin A-C, Jousse C, Muranishi Y, Parry L, Fafournoux P, Bruhat A. Dual role for CHOP in the crosstalk between autophagy and apoptosis to determine cell fate in response to amino acid deprivation. Cell Signal 2014; 26:1385-91. [PMID: 24657471].

26. Gurlo T, Rivera JF, Butler AE, Cory M, Hoang J, Costes S, Butler PC. CHOP contributes to, but is not the only mediator of, IAPP induced β-cell apoptosis. Mol Endocrinol 2016; 30:446-54. [PMID: 26900721].

27. Yu Z, Wang AM, Adachi H, Katsuno M, Sobue G, Yue Z, Robins DM, Lieberman AP. Macroautophagy is regulated by the UPR-mediator CHOP and accentuates the phenotype of SBMA mice. PLoS Genet 2011; 7:e1002321-[PMID: 22022281].

28. Lichtenstein A, Minogue PJ, Beyer EC, Berthoud VM. Autophagy: a pathway that contributes to connexin degradation. J Cell Sci 2011; 124:910-20. [PMID: 21378309].

29. Berthoud VM, Gao J, Minogue PJ, Jara O, Mathias RT, Beyer EC. The connexin50D47A mutant causes cataracts by calcium precipitation. Invest Ophthalmol Vis Sci 2019; 60:2336-46. [PMID: 31117126].

30. Sathyanarayana P, Dev A, Fang J, Houde E, Bogacheva O, Bogachev O, Menon M, Browne S, Pradeep A, Emerson C, Wojchowski DM. EPO receptor circuits for primary erythroblast survival. Blood 2008; 111:5390-9. [PMID: 18349318].

31. Ariyama Y, Shimizu H, Satoh T, Tsuchiya T, Okada S, Oyadomari S, Mori M, Mori M. *Chop*-deficient mice showed increased adiposity but no glucose intolerance. Obesity (Silver Spring) 2007; 15:1647-56. [PMID: 17636082].

32. Marciniak SJ, Yun CY, Oyadomari S, Novoa I, Zhang Y, Jungreis R, Nagata K, Harding HP, Ron D. CHOP induces death by promoting protein synthesis and oxidation in the stressed endoplasmic reticulum. Genes Dev 2004; 18:3066-77. [PMID: 15601821].

33. Chang CJ, Shen BJ, Lee SC. Autoregulated induction of the acute-phase response transcription factor gene, *agp/ebp.* DNA Cell Biol 1995; 14:529-37. [PMID: 7598808].

34. Sylvester SL, ap Rhys CMJ, Luethy-Martindale JD, Holbrook NJ. Induction of *GADD153*, a CCAAT/enhancer-binding protein (C/EBP)-related gene, during the acute phase response in rats. Evidence for the involvement of C/EBPs in regulating its expression. J Biol Chem 1994; 269:20119-25. [PMID: 8051100].

35. Alge CS, Priglinger SG, Neubauer AS. Retinal pigment epithelium is protected against apoptosis by αB-crystallin. Invest Ophthalmol Vis Sci 2002; 43:3575-82. [PMID: 12407170].

36. Dasgupta S, Hohman TC, Carper D. Hypertonic stress induces αB-crystallin expression. Exp Eye Res 1992; 54:461-70. [PMID: 1381680].

37. de Jong WW, Leunissen JAM, Voorter CEM. Evolution of the α-crystallin/small heat-shock protein family. Mol Biol Evol 1993; 10:103-26. [PMID: 8450753].

38. Goldfarb LG, Vicart P, Goebel HH, Dalakas MC. Desmin myopathy. Brain 2004; 127:723-34. [PMID: 14724127].

39. Dou G, Sreekumar PG, Spee C, He S, Ryan SJ, Kannan R, Hinton DR. Deficiency of αB crystallin augments ER stress-induced apoptosis by enhancing mitochondrial dysfunction. Free Radic Biol Med 2012; 53:1111-22. [PMID: 22781655].

40. Shin J-H, Kim S-W, Lim C-M, Jeong J-Y, Piao C-S, Lee J-K. αB-crystallin suppresses oxidative stress-induced astrocyte apoptosis by inhibiting caspase-3 activation. Neurosci Res 2009; 64:355-61. [PMID: 19379782].

41. Kamradt MC, Chen F, Cryns VL. The small heat shock protein *α*B-crystallin negatively regulates cytochrome *c*- and caspase-8-dependent activation of caspase-3 by inhibiting its autoproteolytic maturation. J Biol Chem 2001; 276:16059-63. [PMID: 11274139].

Articles are provided courtesy of Emory University and the Zhongshan Ophthalmic Center, Sun Yat-sen University, P.R. China. The print version of this article was created on 3 October 2019. This reflects all typographical corrections and errata to the article through that date. Details of any changes may be found in the online version of the article.